ISSN: 2664-9640

An UAV-assisted Dynamic Vessel Guidance Route Planning Method for Intelligent Port Navigation Considering Real-time Environmental Evolution

Kai Ma*, Wei Pan

Institute for Big Data Research, Liaoning University of International Business and Economics, Dalian 116052, China

*Corresponding author email: makai@luibe.edu.cn

Abstract

Port traffic changes on a time scale that is poorly served by fixed sensors and precomputed routes. We therefore formulate vessel guidance as a repeatedly updated planning problem and use an unmanned aerial vehicle (UAV) to supply local observations when conventional sources are delayed or incomplete. Electronic navigational chart (ENC) constraints, automatic identification system (AIS) reports, and UAV detections are registered in a time-indexed representation of the navigation area. This representation drives an ECNA-based collision-risk term within the route optimizer, while a feedback loop revises only those route segments affected by new observations. In the simulation case, the resulting route is 0.57% longer than the geometric shortest path but is smoother and remains computable at millisecond scale. Adding UAV observations raises detection coverage from 72.0% to 96.4% and lowers the reported collision-risk index from 0.38 to 0.12. These results indicate that mobile aerial sensing can make port guidance more responsive without sacrificing online computational feasibility.

Keywords

UAV-assisted Navigation; Intelligent Port; Vessel Guidance; Dynamic Environment Modeling; Collision Risk Assessment; Route Planning.

1. Introduction

1.1. Background of Intelligent Port Navigation

Growth in cargo movement is changing the role of a port from a collection of largely independent operating facilities into a data-connected transport node. In this setting, artificial intelligence, Internet of Things devices, and large-scale data analysis are used to coordinate operations rather than merely automate individual tasks. The smart-port framework of Molavi et al. links these technologies to automation, information integration, and operational optimization [1].

A parallel change is occurring on board ships. Maritime autonomous surface ships (MASS) move perception, decision, and control functions from direct human operation toward automated or remotely supervised processes [2–4]. This shift does not remove navigational risk; it changes the way risk must be recognized and managed. Kujala et al. accordingly identified unmanned operation as a new challenge for both risk assessment and maritime safety governance [2].

Ports are a particularly demanding setting for such vessels. Restricted channels, closely spaced traffic, temporary controls, and routine operational changes can invalidate a route even when its geometry was feasible at the time of planning. Safe guidance must therefore use more than a static chart. It must observe the current scene, interpret how it is changing, and revise the planned movement when necessary. This need is consistent with the importance assigned to trajectory prediction by Murray and Perera and to situation awareness by Porathe et al. [3,4]. The present work connects these requirements in a single perception-modeling-planning loop.

1.2. Limitations of Existing Vessel Guidance and Route Planning Methods

Prior work provides substantial foundations in traffic observation, collision assessment, and route search, but these topics are often treated as separate stages. That separation becomes problematic in a port, where the usefulness of a risk estimate or optimized path depends on how recently the environment was observed. The central limitation is thus not the absence of planning algorithms; it is the weak feedback between perception, risk calculation, and route revision.

AIS is widely used because it supplies vessel identity and motion reports over broad areas [5,6]. Yang et al. used such records to examine traffic behavior, while Silveira et al. demonstrated their value in traffic-pattern and collision-risk analysis [5,6]. Nevertheless, AIS is a self-reported source with finite update intervals and uneven availability. A newly appearing obstacle, a non-reporting craft, or a short-lived local restriction may therefore be absent from the data available to a planner.

Ship-routing studies have applied deterministic search, ant-colony methods, and evolutionary optimization to route construction [7–10]. Most formulations, however, solve against an environment specified before the search begins. Re-running such a formulation is possible, but the formulation itself does not explain how changes are detected, which route portion should be replaced, or how observation and replanning should be coordinated online.

Ship-domain and collision-index models add safety information to a route calculation [11–13]. Empirical and dynamic domains, for example, represent the space a vessel requires more realistically than a fixed circular buffer [11–13]. Their use is still commonly centered on a single encounter or on an offline traffic record. A practical guidance system must carry the resulting risk information forward into the route cost and refresh it as relative motion changes.

An aerial platform can fill part of this observation gap. UAVs can be repositioned rapidly and can view a local water area at higher spatial resolution than many fixed installations. Maritime UAV research has largely emphasized surveillance, target monitoring, and communication support; comparatively little attention has been given to using the aircraft as a sensing participant in a vessel-guidance feedback loop [15]. This motivates the combined architecture developed here.

1.3. Research Motivation and Contributions

This paper investigates whether a mobile aerial observer can make route guidance responsive to changes that occur after an initial path has been issued. The proposed method couples UAV observations with ENC and AIS inputs, reconstructs the local environment as a time-dependent model, evaluates vessel interactions with ECNA, and revises the route through a risk-aware optimizer. The design treats sensing and planning as mutually dependent operations rather than as independent modules.

The specific contributions are fourfold:

(1) We define a cooperative guidance architecture in which the UAV acts as a relocatable perception node rather than only as a communications relay.

(2) ENC constraints, AIS reports, and UAV detections are fused into a time-indexed description that separates fixed chart features from objects whose states must be refreshed.

(3) ECNA interaction risk is embedded in a route objective together with travel and environmental-change costs, so feasibility and efficiency are evaluated in the same optimization.

ISSN: 2664-9640

(4) An event-triggered update procedure retains unaffected route segments and recalculates the portion exposed to a newly detected hazard or constraint.

Section 2 describes the guidance architecture and sensing loop. Sections 3 and 4 develop the evolving environment representation and risk-aware optimization model, respectively. Section 5 gives the online planning procedure, Section 6 specifies the simulation design, and Section 7 interprets the results. Section 8 closes the paper with limitations and future work.

2. UAV-assisted Intelligent Vessel Guidance Framework

2.1. System Architecture

The system is organized around a feedback path from observation to route execution. Shore facilities and onboard sensors remain available, but a UAV is added as a movable observation point whose position can follow the area most relevant to the guided vessel. Measurements from all sources are reconciled before the navigation scene is reconstructed. Risk calculation and route search then operate on the same updated scene, and the selected waypoints are returned to the vessel. In this way, a change observed from the air can affect a guidance decision without waiting for the entire route to be planned again from static inputs.

Fig. 1 groups these functions into four layers. The perception layer receives raw ENC, AIS, and aerial data; the fusion and modeling layer resolves them into a common environmental state; the decision layer evaluates risk and selects a route; and the execution layer communicates guidance and receives feedback. The layer boundaries identify the information passed between functions rather than separate, one-way processing stages.

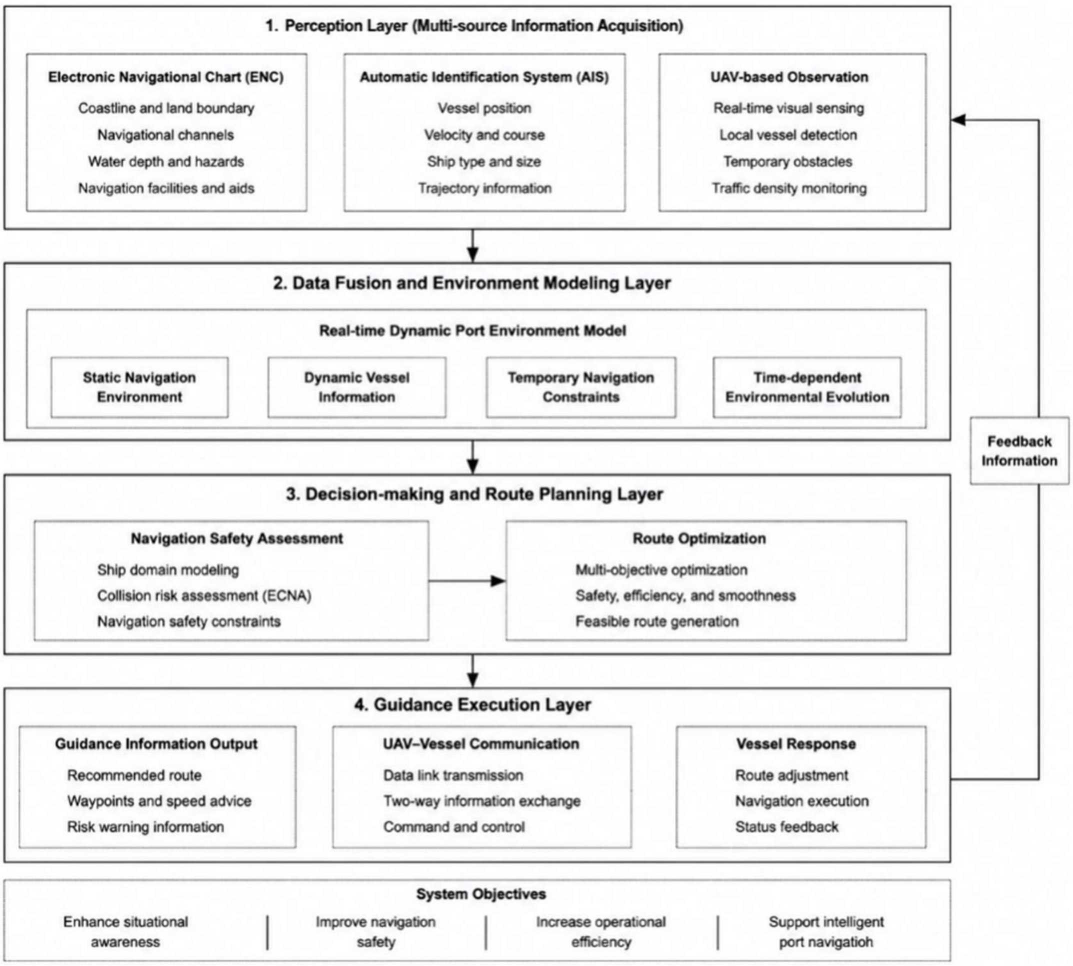

Fig. 1 Overall architecture of UAV-assisted intelligent vessel guidance system

ISSN: 2664-9640

2.2. UAV-based Sensing and Vessel Guidance Mechanism

The quality of a guidance decision is bounded by the age and spatial coverage of its observations. Shore stations, onboard instruments, and AIS provide essential information, yet blind areas and reporting intervals can be consequential in a confined channel [5,6]. The UAV is used where this local deficit is greatest, supplying an additional view that can be redirected as the vessel proceeds.

During a guidance cycle, the UAV observes vessel movements, temporary obstacles, and changes in traffic concentration. Detections are associated with AIS tracks when a match exists; unmatched observations remain as locally detected objects. The fused state then replaces the corresponding part of the environmental model. Thus, the aerial data do not form a separate map but amend the navigation state used by the optimizer.

The information flow in Fig. 2 is cyclical: sensing is followed by fusion, risk evaluation and route selection, transmission to the vessel, and observation of the resulting scene. A later observation may confirm the current route or trigger a local revision. This recurring test is the mechanism by which the system responds to conditions that were not present at departure.

Accordingly, cooperation refers to more than data delivery. Vessel motion changes what the UAV should observe, and the next aerial observation may in turn change the route issued to the vessel.

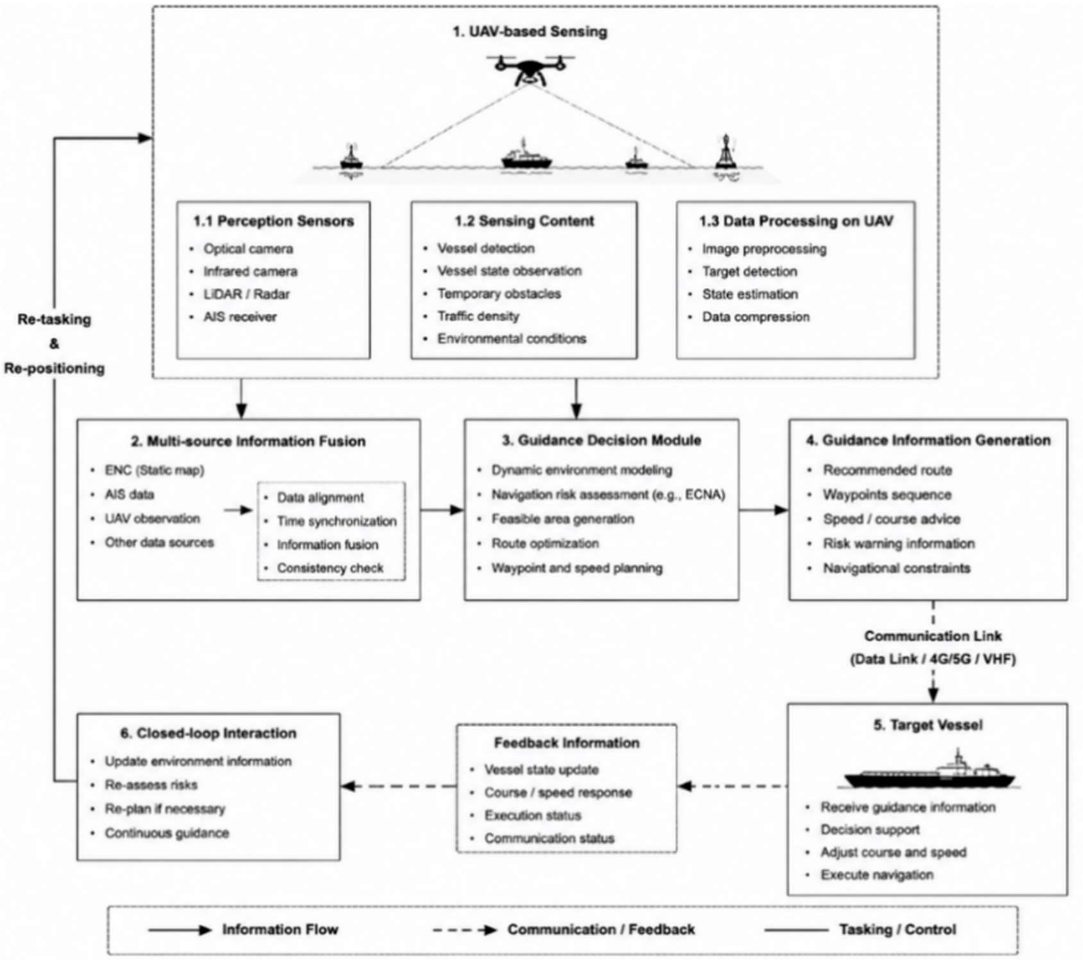

Fig. 2 UAV-based sensing and vessel guidance mechanism

3. Real-time Dynamic Port Environment Modeling

A port map used for online guidance must distinguish enduring constraints from states that may change during a voyage. Coastlines and charted restricted water normally vary slowly, whereas vessel positions and temporary controls can change within minutes. We represent these two classes separately and update only the dynamic class when new AIS or UAV measurements arrive. Fig. 3 summarizes the acquisition, association, and reconstruction sequence.

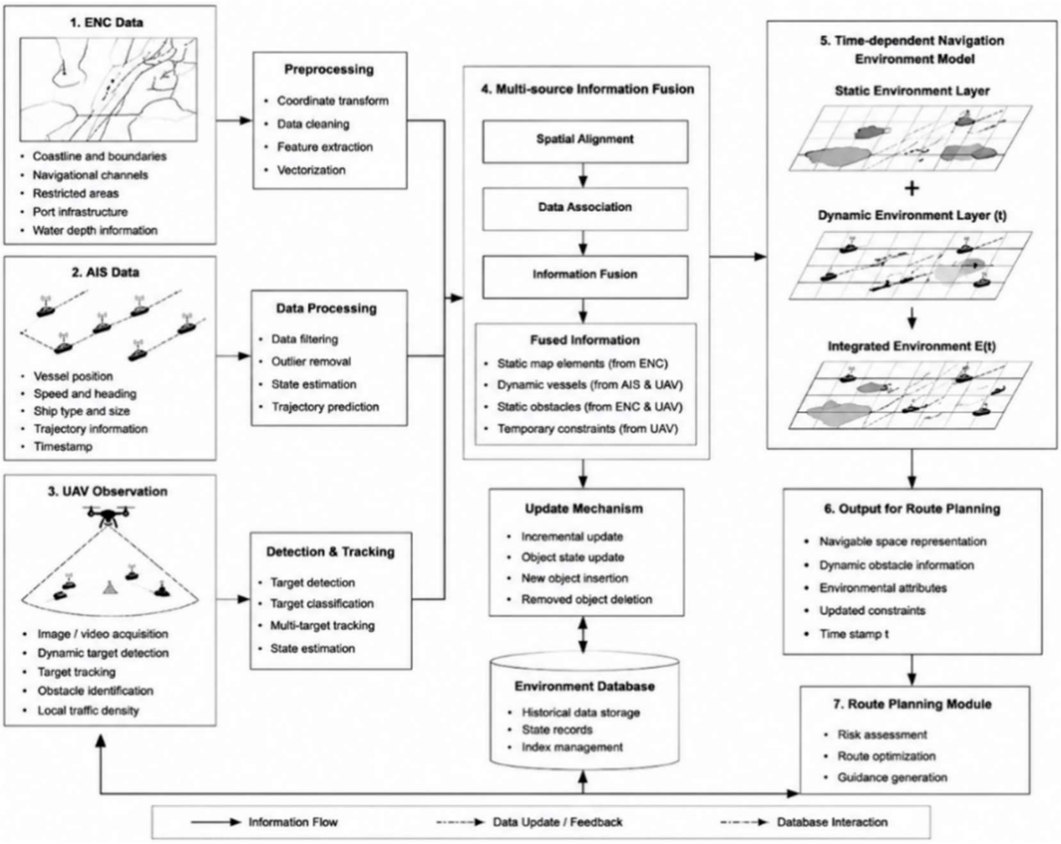

Fig. 3 Workflow of real-time dynamic port environment reconstruction

3.1. Multi-source Environmental Data Acquisition

Three sources contribute different kinds of evidence. ENC supplies the geospatial reference and charted restrictions; AIS supplies identified vessel states; and the UAV supplies local detections, including objects that are absent from the current AIS picture. Their roles are complementary, so the fusion process preserves source type and observation time rather than treating all records as equivalent [5,6,15].

ENC features establish the static layer. Coastlines, channel limits, depth restrictions, prohibited areas, and port structures are converted to geometric constraints in the planning coordinates. Their union removes non-navigable space before any moving-object risk is considered.

For the dynamic layer, an AIS report for vessel i is stored as a state vector containing position, speed, course, and identifier:

$$S_i(t) = [x_i(t), y_i(t), v_i(t), \psi_i(t), m_i] \tag{1}$$

Here, the two position terms locate vessel i, the speed and heading terms describe its reported motion, and the final term retains the vessel identifier.$x_i(t) y_i(t) i v_i(t) \psi_i(t) m_i$

ISSN: 2664-9640

Successive AIS states provide the main track history for reporting vessels. They support motion extrapolation and encounter calculations, but each state is time stamped so that an old report is not interpreted as a current observation.

The aerial stream is used to correct the local picture when AIS coverage is delayed, incomplete, or unavailable. Detected non-reporting vessels and temporary objects are inserted into the dynamic layer, while matches to existing AIS tracks update rather than duplicate those tracks. Combining the wide-area continuity of AIS with the UAV's local detail yields a navigation state that can be refreshed as events occur.

3.2. UAV-based Dynamic Target Detection and Tracking

UAV video is processed in three operations: frame acquisition, object recognition, and motion estimation. The aircraft is treated as a mobile sensor with a known pose, allowing image detections to be projected into the navigation coordinate system. This step is necessary before an aerial detection can be compared with an AIS track or used by the route model.

Frames collected over the area of interest reveal small craft, temporary obstructions, and local traffic organization that may be poorly resolved by fixed monitoring. The imagery is used only after georeferencing and time synchronization with the other sources.

Each recognized moving object is assigned a position, estimated speed, and direction state:

$$O_j(t) = [x_j(t), y_j(t), v_j(t), \theta_j(t)] \tag{2}$$

The first two components give the target position; the remaining components record estimated velocity and direction.$x_j(t) y_j(t) v_j(t) \theta_j(t)$

Track association links detections across adjacent frames. The resulting short trajectories reduce frame-to-frame noise and provide a motion estimate even when no AIS identity is available. Where an AIS state and an aerial track agree spatially and kinematically, they are merged as observations of one vessel; otherwise, the aerial track is retained as an independent object.

This procedure adds value in two distinct ways. It extends coverage into local blind areas, and it shortens the time between an unexpected event and its representation in the planner. The second property is especially important here because route revision depends on detecting change soon enough for the vessel to respond.

3.3. Time-dependent Navigation Environment Reconstruction

Let the navigation scene at time t comprise a static chart layer and a dynamic interaction layer. The chart layer is held fixed over a guidance run unless an explicit restriction update is received. Vessel tracks, detected objects, traffic concentration, and temporary controls belong to the dynamic layer and carry their most recent observation time. This separation avoids reconstructing unchanged chart geometry at every cycle.

The static layer defines the base navigable set from coastline, channel, depth, and restriction polygons. The dynamic layer overlays predicted vessel occupancy and the current geometry of temporary hazards. Because each dynamic object is stored with its motion state, its occupied or risky region can be advanced to the route-evaluation time rather than frozen at the last measurement.

The complete scene at time t is written as:

$$E(t) = \{E_s, E_d(t)\} \tag{3}$$

ISSN: 2664-9640

where the first term denotes the static constraints and the second collects time-varying environmental elements.$E_s E_d(t)$

For computation, the navigable set is discretized as connected nodes and edges. Nodes store accessibility, local risk, and obstacle status; edges record feasible motion between neighboring states. An incoming AIS report or UAV observation changes only the nodes and edges within its affected region, according to the incremental update:

$$E(t + \Delta t) = F(E(t), D(t + \Delta t)) \tag{4}$$

In this expression, the new-information term contains observations received after the preceding update. The reconstructed graph is therefore both time referenced and economical to refresh, providing the state used by the risk and routing calculations that follow.$D(t + \Delta t)$

4. Risk-aware Vessel Guidance Optimization Model

In dynamic port environments, vessel guidance requires more than geometric feasibility, as navigation safety is continuously influenced by vessel interactions, restricted areas, and evolving environmental conditions. Therefore, an effective guidance strategy should simultaneously consider navigation constraints, collision risks, and operational efficiency.

Based on the real-time dynamic port environment model developed in Section 3, this study establishes a risk-aware vessel guidance optimization model. The proposed model integrates dynamic navigation safety constraints, ECNA-based collision risk assessment, and multi-objective route optimization to generate safe and adaptive guidance routes. Unlike conventional approaches that assume static navigation conditions, the proposed model incorporates time-dependent environmental information and dynamic risk variations into the optimization process.

The proposed optimization model consists of three main components. First, a dynamic navigation safety constraint model is developed to determine feasible navigation regions by considering both static geographic restrictions and dynamic obstacle avoidance requirements. Second, an ECNA-based collision risk assessment model is introduced to quantify interaction risks between the target vessel and surrounding dynamic objects. Finally, a multi-objective guidance route optimization model is formulated to balance navigation safety and route efficiency.

4.1. Dynamic Navigation Safety Constraint Model

In intelligent port navigation, a feasible guidance route should satisfy both geographic constraints and dynamic safety requirements. Based on the reconstructed environment model in Section 3, the navigation space consists of static geographic features and dynamic maritime objects. Static constraints include coastline boundaries, shallow water areas, restricted navigation zones, and port infrastructures, while dynamic constraints are introduced by moving vessels and temporary obstacles. Therefore, the feasible navigation region is first determined according to static environmental constraints. Let the original navigation space be defined as:

$$\Omega = \{(x, y) \mid (x, y) \in R^2\} \tag{5}$$

where (x, y) represents the position in the navigation coordinate system. The static obstacle region extracted from ENC data is defined as:

ISSN: 2664-9640

$$\Omega_s = \{O_1, O_2, \dots, O_n\} \tag{6}$$

where O_i represents the i-th static forbidden area. Therefore, the static feasible navigation region can be expressed as:

$$\Omega_f = \Omega - \Omega_s \tag{7}$$

However, static constraints alone cannot guarantee navigation safety in dynamic port environments. Moving vessels introduce additional collision risks, requiring dynamic safety boundaries. For each surrounding vessel i, a dynamic safety domain is constructed according to its motion state:

$$D_i(t) = f(V_i, \psi_i, L_i, B_i) \tag{8}$$

where V_i represents vessel speed, ψ_i represents heading angle, and L_i and B_i denote vessel length and breadth, respectively. The dynamic obstacle region is defined as:

$$\Omega_d(t) = \bigcup_{i=1}^{N} D_i(t) \tag{9}$$

where N represents the number of surrounding vessels. By integrating static and dynamic constraints, the time-dependent feasible navigation region becomes:

$$\Omega(t) = \Omega_f - \Omega_d(t) \tag{10}$$

The established navigation constraint model ensures that generated guidance routes satisfy both static geographic restrictions and dynamic safety requirements by avoiding fixed obstacles and time-varying collision-risk regions. Furthermore, with continuous updates from UAV sensing and AIS information, the dynamic constraint model can be adaptively adjusted according to environmental changes, enabling real-time route modification under evolving port navigation conditions.

4.2. ECNA-based Dynamic Collision Risk Assessment

Although dynamic safety domains can provide basic collision avoidance constraints, they cannot quantitatively describe the degree of collision risk during vessel interactions. Therefore, this study introduces the Especial Cautious Navigation Angle (ECNA) model to evaluate dynamic collision risks among vessels. The basic principle of ECNA is that collision risk is associated with the relative motion relationship between the own ship and target vessels. Considering the relative velocity vector between two vessels:

$$V_r = V_t - V_o \tag{11}$$

where V_t and V_o represent the velocities of the target vessel and own vessel, respectively. The collision risk region is determined by the relative motion geometry and the angular distribution of dangerous navigation directions. The ECNA model defines a risk-sensitive angular domain:

$$\Theta = [\theta_L, \theta_R] \tag{12}$$

ISSN: 2664-9640

where θ_L and θ_R represent the left and right boundaries of the risk angle. Different from conventional collision indicators such as DCPA and TCPA, which mainly describe encounter severity at specific moments, ECNA evaluates collision risk from the perspective of continuous angular interaction between vessels [7,8]. The risk contribution of each navigation direction is calculated as:

$$\zeta(\theta) = \frac{V_r(\theta)}{D(\theta)} \tag{13}$$

where $D(\theta)$ represents the relative distance corresponding to navigation direction θ. The integrated collision risk index is then obtained as:

$$\chi = \int_{\theta_L}^{\theta_R} \zeta(\theta) d\theta \tag{14}$$

where χ represents the collision risk value. For multiple surrounding vessels, the overall navigation risk is calculated as:

$$\chi_{sum} = \sum_{i=1}^{N} w_i \chi_i \tag{15}$$

where w_i represents the weighting coefficient determined by factors such as TCPA, relative velocity, and encounter situation. The ECNA-based risk assessment provides a continuous and quantitative description of vessel interaction risks. By incorporating the risk index into route optimization, the proposed guidance model can avoid dangerous areas while maintaining route efficiency.

4.3. Multi-objective Guidance Route Optimization Model

Based on the established dynamic navigation constraints and ECNA-based collision risk evaluation, a multi-objective optimization model is formulated to generate safe and efficient guidance routes. The optimization process considers both navigation safety and route efficiency, while adapting to time-varying environmental conditions. A candidate guidance route is represented as a sequence of connected waypoints:

$$P = \{p_1, p_2, \ldots, p_m\} \tag{16}$$

where p_m represents the waypoint of the route. The optimization objective considers three factors: Route efficiency, Navigation safety, Environmental adaptability. The route length objective is defined as:

$$J_1 = \sum_{k=1}^{m-1} \| p_{k+1} - p_k \| \tag{17}$$

The collision risk objective is defined as:

$$J_2 = \sum_{k=1}^{m} \chi(p_k) \tag{18}$$

where $\chi(p_k)$ represents the risk value at waypoint p_k. To improve adaptability under dynamic environments, an environmental change cost is introduced:

ISSN: 2664-9640

$$J_3 = \Delta E(t) \tag{19}$$

where $\Delta E(t)$ represents environmental variation during route execution. Therefore, the comprehensive optimization function is formulated as:

$$\min F = \alpha J_1 + \beta J_2 + \gamma J_3 \tag{20}$$

where α, β, and γ are weighting coefficients representing the importance of route efficiency, safety, and environmental adaptability. The optimization problem is subject to:

$$P \subseteq \Omega(t) \tag{21}$$

which ensures that the generated route remains within the dynamically feasible navigation space. By solving the multi-objective optimization problem, the optimal guidance route is obtained:

$$P^* = \operatorname{argmin}(F) \tag{22}$$

The proposed model enables vessels to select safe and efficient navigation routes while continuously adapting to dynamic changes in port environments.

5. UAV-assisted Dynamic Guidance Route Planning Algorithm

A path that is safe at departure can lose that property before the vessel reaches its destination. A crossing vessel may alter course, an unreported craft may enter the channel, or a temporary exclusion zone may be imposed. Section 4 provides a route objective for a specified environmental state; this section specifies when that state is reconsidered and how a revised route is produced while navigation continues.

The online algorithm links three operations: generation of a departure route, event-triggered repair of that route, and repositioning of the assisting UAV. Each operation uses the same environmental and ECNA risk representation. The distinction from a static planner lies in this recurring loop: observations are tested against the current route, and only a material change invokes optimization.

The procedure begins with a graph built from the reconstructed environment. The risk-aware search returns an initial waypoint sequence. While the vessel follows it, the UAV samples the nearby scene and forwards associated detections. If the new state changes a safety constraint or raises interaction risk beyond its threshold, the route interval intersecting the change is searched again. In parallel, the UAV location is adjusted to preserve useful viewing geometry and communication quality.

5.1. Initial Guidance Route Generation

Before departure, chart restrictions and the available dynamic-object states are projected into the feasible set. This set is discretized into a graph in which vertices denote admissible vessel states and edges denote permitted transitions:

$$G = (V, E) \tag{23}$$

Here, the vertex set contains feasible navigation nodes and the edge set contains connections between adjacent nodes. A node stores the following environmental attributes:VE

$$v_i = (x_i, y_i, c_i, r_i) \quad (24)$$

The coordinate terms locate the node, while the remaining entries record traversal cost and local collision risk. For adjacent nodes, the transition cost is:x_i $y_i c_i r_i$

$$C_{ij} = \lambda_1 d_{ij} + \lambda_2 \chi_{ij} + \lambda_3 \Delta e_{ij} \quad (25)$$

The three terms measure distance, ECNA risk, and sensitivity to environmental variation, respectively. Summing this cost along a candidate sequence gives the initial route problem:$d_{ij} \chi_{ij} \Delta e_{ij}$

$$P_0 = \mathrm{argmin} \sum C_{ij} \quad (26)$$

Unlike a purely geometric shortest path, this search may accept a modest detour to avoid an interaction-risk region. Once selected, the waypoints are sent to the vessel and stored as the reference route. They remain valid until later observations show that a route segment violates a constraint or exceeds the selected risk tolerance.

5.2. Real-time Route Updating Mechanism

At each update cycle, the latest observations are compared with the environmental state used for the current route. The comparison follows a perception-decision-update loop. No route change is made when differences are immaterial; this prevents repeated optimization in response to measurement noise and small routine movements.

$$E(t) \rightarrow \Delta E(t) \rightarrow P(t + \Delta t) \quad (27)$$

The change term measures the difference between the current state and the newly observed state. Replanning is triggered if a new obstacle appears in the navigation area, a surrounding track departs materially from its predicted trajectory, ECNA risk crosses the safety threshold, or a temporary restriction alters the feasible set [14]. These conditions tie computation to changes that can affect route validity.$E(t) \Delta E(t)$

For a quantitative trigger, environmental variation is summarized by:

$$\eta = w_1 \Delta N + w_2 \Delta R + w_3 \Delta O \quad (28)$$

The indicator combines changes in vessel count, collision risk, and obstacle state. Once its decision condition is met, the affected route interval is replaced by the solution:$\Delta N \Delta R \Delta O \eta > \eta_{th}$

$$P_{new} = \mathrm{argmin} F(P \mid E(t + \Delta t)) \quad (29)$$

The objective is the multi-criteria function from Section 4. Nodes before and after the affected interval are retained as boundary conditions, so the algorithm repairs a portion of the route

ISSN: 2664-9640

rather than solving the complete origin-to-destination problem again. This is the principal means of controlling update time.F

5.3. UAV-Vessel Cooperative Optimization

The aerial platform must remain useful as both a sensor and a communication node, but the best viewing location is not necessarily the least costly flight position. We therefore select its deployment by trading sensing coverage and link quality against energy use [15]. The UAV position is represented as:

$$U(t) = (x_u , y_u , h_u) \tag{30}$$

The first two variables are horizontal coordinates, and the third is altitude.$x_u y_u h_u$

Three quantities enter the deployment objective:

(1) the fraction and quality of sensing coverage;

(2) the reliability of the UAV-vessel communication link; and

(3) the energy required to occupy and move between candidate positions.

Their weighted cooperative cost is:

$$J_U = \alpha C_s + \beta C_c + \gamma C_e \tag{31}$$

The terms denote coverage loss, communication cost, and energy consumption. Coverage is evaluated through the UAV-to-area or UAV-to-vessel distance:$C_s C_c C_e$

$$C_s = f(d_u) \tag{32}$$

where the distance term is computed for the guided vessel and the relevant observation region. Communication reliability is likewise modeled as a function of separation and environmental interference:d_u

$$C_c = f(R_{uv}) \tag{33}$$

where the reliability variable describes the UAV-vessel link. The deployment decision is then written as:R_{uv}

$$U^* = \mathrm{argmin} J_U \tag{34}$$

subject to:

$$d_{min} < d_u < d_{max} \tag{35}$$

The constraints enforce minimum coverage and link reliability. As the vessel and surrounding traffic move, solving this problem relocates the aerial viewpoint toward the part of the scene that most affects guidance, subject to the cost of doing so.

Algorithm 1 combines environment updates, ECNA evaluation, local route repair, and UAV deployment in one loop. Its input-output statement also makes explicit that the procedure returns both a vessel route and an aerial position.

ISSN: 2664-9640

Algorithm 1. UAV-assisted dynamic guidance route planning algorithm

Input:	ENC data E_s AIS data A(t) UAV observations U(t) Initial vessel state S0
Output:	Guidance route P* UAV position U*
	Acquire multi-source environmental information
	Generate dynamic environment model E(t)
	Initialize guidance route P0
	while vessel is navigating do
	Update environmental information using UAV
	Calculate ECNA-based collision risk
	if risk > threshold then
	Update route segments
	end if
	Optimize UAV position
	Send guidance information to vessel
	end while
	return P*, U*

6. Case Study and Experimental Design

Evaluation uses a simulated port scene containing charted boundaries, fixed obstacles, moving vessels, and a temporary restriction. The design is intended to expose the planner to both geometric constraints and changes that arise after the initial route has been calculated. Fig. 4 shows the common spatial setting used for the experiments; individual scenarios vary the number and behavior of dynamic objects within it.

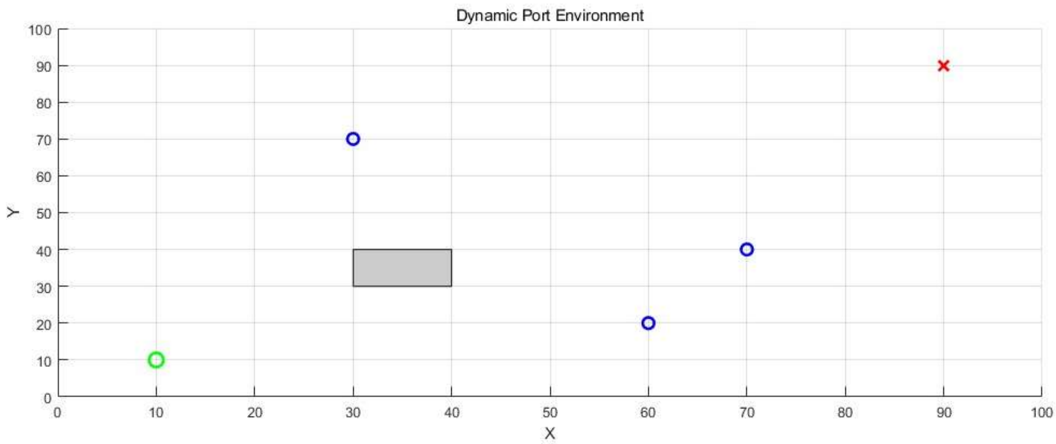

Fig. 4 Dynamic Port Environment

Chart-derived boundaries and obstacle polygons define the base feasible region. Vessel targets are then assigned positions, velocities, and encounter geometries that change over the run. Keeping the geographic layer common while varying the dynamic layer allows route changes to be attributed to traffic and restriction events rather than to a different map.

ISSN: 2664-9640

6.1. Study Area and Data Preparation

The selected test area represents a confined port approach with channel boundaries, irregular coastline geometry, and several interacting vessels. It is a representative simulation setting rather than a claim of full operational replication; its purpose is to test the closed-loop behavior under controlled changes.

ENC features are converted to coast, channel, restriction, and shallow-water constraints. AIS trajectories supply the reported position, speed, course, and recent history of each simulated vessel. UAV observations are generated for the aircraft's local field of view and include detections of new vessels and temporary obstacles. All records are time synchronized before fusion.

The resulting data produce a sequence of environmental states rather than one fixed map. This sequence is supplied to the online planner so that the response to each introduced event can be measured.

6.2. Experimental Scenarios

Table 1 defines four cases of increasing functional scope. The first tests route feasibility in an otherwise stable environment; the second adds multiple encounter types; the third introduces changes during navigation; and the fourth activates the complete UAV-assisted loop. Using nested cases separates the contribution of individual modules from the behavior of the integrated system.

Table 1. Experimental Scenario

Scenario	Expression	Evaluation focus
Static Navigation Environment	This scenario considers a relatively stable port environment without significant dynamic changes. Only static geographic constraints and normal vessel traffic information are included.	route feasibility; navigation distance; computational efficiency.
Multi-vessel Interaction Scenario	This scenario introduces multiple surrounding vessels with different motion states, including crossing, overtaking, and approaching encounters.	ECNA-based collision risk assessment; dynamic safety constraint effectiveness; multi-vessel guidance capability.
Dynamic Environmental Evolution Scenario	This scenario considers continuously changing navigation conditions.	real-time perception capability; route updating mechanism; adaptability to environmental evolution.
UAV-assisted Cooperative Guidance Scenario	This scenario evaluates the complete UAV-assisted guidance process.	UAV sensing coverage; communication effectiveness; cooperative guidance performance.

6.3. Benchmark Algorithms

Four outcome groups are recorded: route length and computation time, collision-risk behavior, response to imposed environmental changes, and the effect of UAV observations. The shortest-path, A*, and ant-colony optimization (ACO) routes provide reference behaviors with different search characteristics. Comparisons use the same map and event schedule wherever the methods permit.

Because the proposed method changes both perception and planning, route geometry alone is insufficient for evaluation. We also report whether hazards are observed, how the risk index responds, and whether the route can be updated within an online time scale. These measures correspond to the information, safety, and computational claims made by the framework.

ISSN: 2664-9640

7. Results and Discussion

7.1. Route Planning Efficiency

Route performance is compared with a geometric shortest path, A*, and ACO. These baselines distinguish the effect of minimum-distance search, constraint-aware graph search, and iterative population-based optimization. The proposed method adds time-varying risk and observation updates to the comparison. Fig. 5 plots the four resulting trajectories, and Table 2 reports length, smoothness, and computation time.

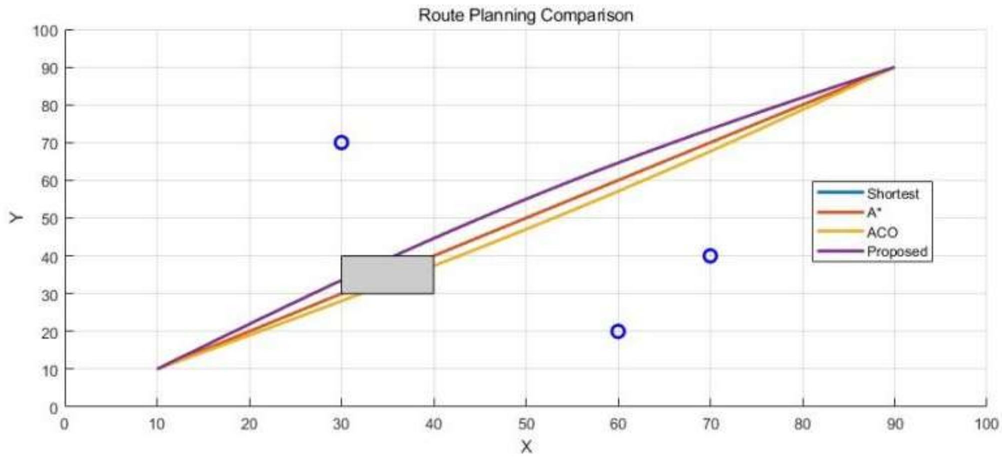

Fig. 5 The generated routes under different planning strategies

The shortest-path result has a length of 88.91 and smoothness of 0.571. It follows the direct geometric solution and therefore provides a useful lower-distance reference, but it contains no mechanism for representing a moving encounter or a newly imposed restriction.

A* returns the same reported length and smoothness in this scene, with computation increasing from 0.001 s to 0.002 s. Its graph search respects the constraints encoded at planning time; however, a changed environment must first be supplied through an external update before the route can respond.

ACO produces a route of 89.36 with smoothness 0.604 and requires 0.003 s. Iterative search improves the trajectory measure relative to the two 88.91-length routes, although repeated optimization adds computation when frequent updates are required.

The proposed trajectory is 89.42 long, has the highest reported smoothness (0.641), and is computed in 0.004 s. In Fig 5 it bends away from regions carrying elevated interaction risk. Thus, its extra length is associated with the safety term rather than with failure to find the geometric minimum.

Table 2. Comparison of route planning performance

Method	Route Length	Route Smoothness	Computational Time(s)
Shortest Path	88.91	0.571	0.001
A*	88.91	0.571	0.002
ACO	89.36	0.604	0.003
Proposed Method	89.42	0.641	0.004

Relative to the shortest-path value, the proposed route adds 0.51 distance units, or approximately 0.57%. That small increase is the measurable price of including dynamic constraints and ECNA risk in the objective.

The smoothness gain is 0.070 over the shortest-path and A* results and 0.037 over ACO. Fewer abrupt directional changes are desirable for vessel execution, although this metric alone does not establish maneuverability under all ship dynamics. All four reported times are in milliseconds; the 0.004 s result therefore leaves substantial room within the simulation's update interval.

7.2. Navigation Safety Improvement

Safety performance is examined through the ECNA values of 20 surrounding vessels. ECNA combines relative position and motion geometry, so targets at similar distances need not receive the same risk value. Fig. 6 gives the distribution, and the scenario-level total is computed as:

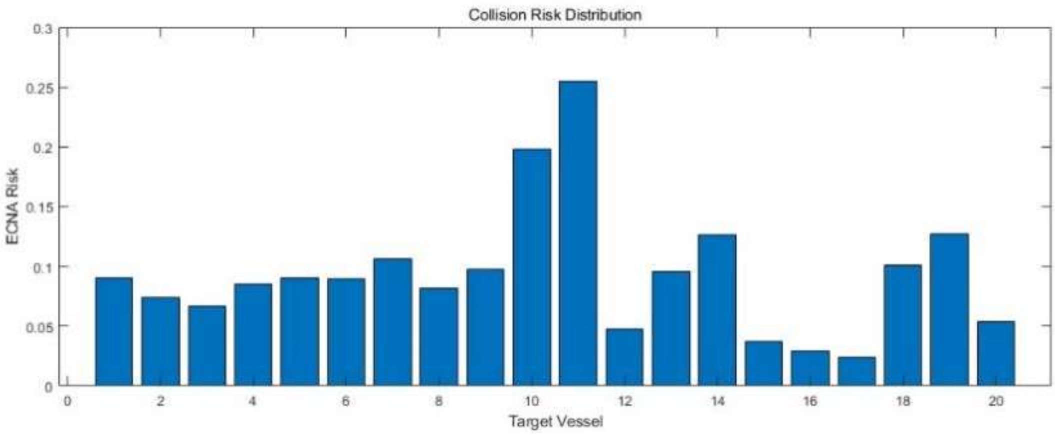

Fig. 6 The collision risk distribution of 20 surrounding vessels

The ECNA risk value is calculated by considering the relative distance and motion characteristics between the own ship and surrounding vessels. A higher ECNA value indicates a higher collision risk level, reflecting a more critical encounter situation. The total collision risk of the navigation scenario is calculated as:

$$R_c = \sum_{i=1}^{N} \chi_i \tag{36}$$

where the summand is the ECNA value assigned to target vessel i.χ_i

The distribution is nonuniform: closer targets with larger relative velocity tend to occupy the upper end, while well-separated or diverging targets contribute less. This ranking is useful to the planner because it identifies which encounter, rather than merely which object, should influence a route segment. A distance-only buffer would not express this angular and kinematic difference. Incorporating ECNA into the edge cost directs the search away from the regions associated with the highest contributions.

7.3. Adaptability to Dynamic Environmental Evolution

Two events are inserted during the run to test online response. At t = 300 s, an additional vessel enters the navigation area; at t = 600 s, a temporary restricted region removes part of the previously feasible space. The first event changes interaction risk, whereas the second changes route feasibility. Fig. 7 plots the risk trace across both events.

ISSN: 2664-9640

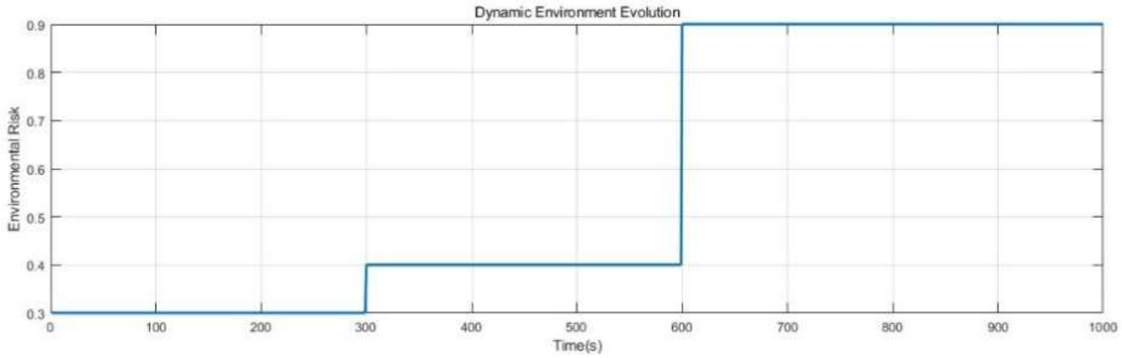

Fig. 7 The variation of environmental risk during the simulation process.

Risk is nearly steady before the first event. The arriving vessel causes an immediate increase because a new relative-motion relationship enters the ECNA calculation. After the observation is fused, the affected route segment is recomputed and the risk declines. The restriction introduced at 600 s produces a different response: nodes inside the new region become infeasible, requiring the route to pass around its boundary.

The experiment therefore tests two distinct functions of the loop: responding to a graded change in encounter risk and responding to a binary loss of navigable space. In both cases, the route is revised from the latest AIS and UAV state rather than from the departure map. This behavior supports the claimed adaptability within the simulated setting; field latency and sensor error remain to be evaluated separately.

7.4. UAV-assisted Guidance Performance

To isolate the sensing contribution, the same guidance process is run with AIS alone and with AIS plus UAV observations. The comparison concerns information available to the planner, not a change in the underlying traffic. Detection coverage and the resulting collision-risk index are reported in Fig 8 and Table 3.

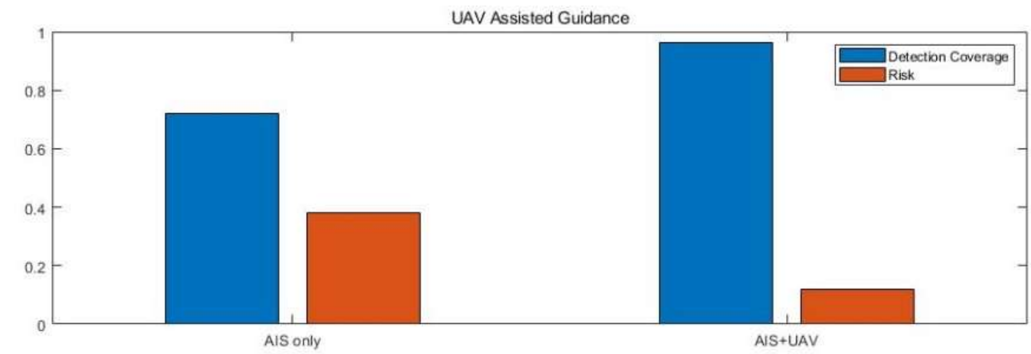

Fig. 8 The comparison results.

Table 3. Performance comparison of UAV-assisted guidance

Configuration	Detection Coverage	Collision Risk
AIS only	72.0%	0.38
AIS + UAV	96.4%	0.12

AIS alone covers 72.0% of the relevant detections and yields a collision-risk value of 0.38. With the UAV stream enabled, coverage rises to 96.4%, a gain of 24.4 percentage points (33.9% relative), while risk falls to 0.12. The paired change is consistent with the planner receiving earlier or more complete information about local hazards.

The largest informational benefit occurs where an AIS message is absent, delayed, or too coarse for the local scene. Aerial detections add nearby vessel motion, temporary objects, and local density changes to the fused state. Once these items are represented, the risk calculation can influence the route before the vessel reaches the affected area.

These results support the UAV's role as a cooperative observation node. They do not, by themselves, quantify weather sensitivity, detection error, or communication outages; those factors should be included in a field-oriented validation.

7.5. Ablation Analysis

An ablation study removes or adds the principal modules in sequence. Fig. 9 compares the baseline planner, dynamic environment reconstruction, reconstruction with ECNA, and the complete configuration with UAV sensing.

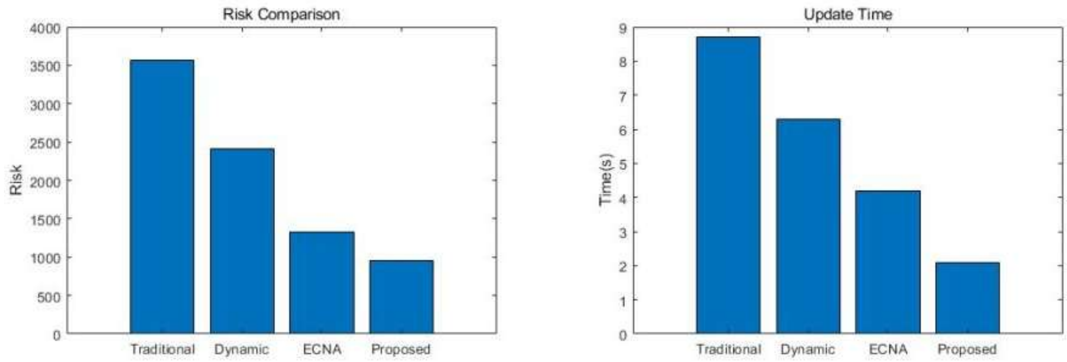

Fig. 9 The comparison results among four models

The baseline performs least well because its input state is not refreshed. Adding environment reconstruction reduces risk by allowing current constraints to enter the route search. ECNA supplies a further reduction by distinguishing encounter severity rather than treating all dynamic objects alike. The final addition of UAV sensing improves the timeliness and local coverage of the state used by both preceding modules.

The staged pattern indicates that no single module accounts for the full result: reconstruction provides an update mechanism, ECNA determines how an interaction should be weighted, and the UAV supplies observations that may otherwise be missing. Their benefits are consequently complementary in this simulation.

8. Conclusion

This work formulated port guidance as an observation-and-replanning loop supported by a mobile aerial sensor. ENC geometry defines the persistent constraints, AIS reports provide identified traffic states, and UAV detections amend the local picture. The fused state is evaluated with ECNA and passed to a multi-criteria route search; when an event affects only part of the route, that part is repaired rather than rebuilding the complete path.

The numerical results illustrate the trade-off produced by this design. The proposed path is 0.57% longer than the shortest geometric route, yet its smoothness increases from 0.571 to 0.641 and its reported calculation time remains 0.004 s. In the sensing comparison, UAV support raises coverage from 72.0% to 96.4% and reduces the collision-risk value from 0.38 to 0.12.

The dynamic tests add a second type of evidence. A vessel introduced at 300 s changes the interaction-risk field, while a restriction introduced at 600 s changes the feasible set. The planner responds to both through the same update loop, showing that risk variation and loss of navigable space need not be handled by separate guidance architectures.

These findings are limited to the constructed simulation and the assumed sensing and communication conditions. They establish algorithmic feasibility, not operational certification. In particular, the present experiment does not reproduce adverse weather, image-detection errors, packet loss, or the maneuvering limits of different vessel classes.

Future experiments will therefore use recorded or live UAV imagery together with larger AIS datasets, introduce observation uncertainty and communication delay, and couple the route output to vessel-specific motion models. Multi-UAV allocation and energy-aware repositioning are further extensions when one aircraft cannot maintain the required view.

Within those limits, the study shows how aerial observation can be integrated directly into the logic of dynamic port route guidance rather than treated as an independent surveillance service.

Acknowledgments

This work was supported by the "Research Project of Liaoning University of International Business and Economics" [2023XJLXYBWT04].

References

[1] Molavi, A., Lim, G., & Race, B. (2020). A framework for building a smart port and smart port index. *International Journal of Sustainable Transportation*, 14, 686–700. https://doi.org/10.1080/15568318.2019.1610919

[2] Kujala, P., Montewka, J., et al. (2017). Towards the assessment of potential impact of unmanned vessels on maritime transportation safety. *Reliability Engineering & System Safety*.

[3] Murray, B., & Perera, L. P. (2018). A data-driven approach to vessel trajectory prediction for safe autonomous ship operations. In *2018 13th International Conference on Industrial and Information Systems (ICDIM)*. https://doi.org/10.1109/ICDIM.2018.8847003

[4] Porathe, T., Prison, J., & Man, Y. (2014). Situation awareness in remote control centres for unmanned ships.

[5] Yang, D., Wu, L., Wang, S., et al. (2019). How big data enriches maritime research – a critical review of Automatic Identification System (AIS) data applications. *Transport Reviews*, 39, 755–773. https://doi.org/10.1080/01441647.2019.1649315

[6] Silveira, P. A. M., Teixeira, A. P., & Soares, C. G. (2013). Use of AIS data to characterise marine traffic patterns and ship collision risk off the coast of Portugal. *Journal of Navigation*, 66(6), 879–898. https://doi.org/10.1017/S0373463313000519

[7] Lazarowska, A. (2016). A new deterministic approach in a decision support system for ship's trajectory planning. *Expert Systems with Applications*, 71, 469–478. https://doi.org/10.1016/j.eswa.2016.11.005

[8] Zaccone, R., & Martelli, M. (2019). A collision avoidance algorithm for ship guidance applications. *Journal of Marine Engineering & Technology*, (1), 1–14. https://doi.org/10.1080/20464177.2019.1685836

[9] Tsou, M. C., & Cheng, H. C. (2013). An ant colony algorithm for efficient ship routing. *Polish Maritime Research*, 20(3), 28–38. https://doi.org/10.2478/pomr-2013-0032

[10] Szlapczynski, R. (2011). Evolutionary sets of safe ship trajectories: A new approach to collision avoidance. *Journal of Navigation*, 64(1), 169–181. https://doi.org/10.1017/S0373463310000238

[11] Yahei, F., Kenichi, et al. (1971). Traffic capacity. *Journal of Navigation*. https://doi.org/10.1017/S0373463300022384

[12] Wang, N. (2013). A novel analytical framework for dynamic quaternion ship domains. *Journal of Navigation*, 66(2), 265–281. https://doi.org/10.1017/S0373463312000483

[13] Hansen, M. G., Jensen, T. K., Lehn-Schjøller, T., et al. (2013). Empirical ship domain based on AIS data. *Journal of Navigation*, 66(6), 931–940. https://doi.org/10.1017/S0373463313000489

[14] Zhang, W., Goerlandt, F., Montewka, J., et al. (2015). A method for detecting possible near miss ship collisions from AIS data. *Ocean Engineering*, 107, 60–69. https://doi.org/10.1016/j.oceaneng.2015.07.046

[15] Nomikos, N., Gkonis, P., Bithas, P., et al. (2022). A survey on UAV-aided maritime communications: Deployment considerations, applications, and future challenges. *IEEE Open Journal of the Communications Society*, 4, 56–78. https://doi.org/10.1109/OJCOMS.2022.3225590